Elucidating Transport-Recombination Mechanisms in Perovskite Solar Cells by Small-Perturbation Techniques

Elena Guillén,[a] *F. Javier Ramos,*[a] *Juan A. Anta,*[b] *Shahzada Ahmad*[a*]

[a]Abengoa Research, C/ Energía Solar nº 1, Campus Palmas Altas, 41014, Sevilla, Spain

[b]Department of Physical, Chemical and Natural Systems, University Pablo de Olavide,41013 Sevilla, Spain

Checking procedure for small perturbation characterization of perovskite solar cells. To ascertain the validity of IMPS measurements we assume that we need to fulfill the same conditions that when carrying out an EIS measurement. There is not a standard experimental protocol for testing the accuracy of an impedance measurement, but it is well known that the following conditions must be fulfilled: linearity, causality and stability.[1] Regarding linearity, the applied AC amplitude must be small enough to assure that the response of the cell is linear. Regarding causality, the AC response of the system must be directly correlated to the AC applied perturbation. Moreover, the cell needs to remain stable along the duration of the measurement. One way of checking stability is measuring a cyclic voltagram before and after the measurement and check if any change is observed. There are also some experimental tests that have been used to check the afore-mentioned conditions fulfilling during EIS measurements: the Lissajous plot and the resolution plot. Lissajous plot is considered obsolete for numeric evaluation of impedance measurements, but still it can be very useful to check linearity. In this plot, the AC current response is plotted versus

the AC input potential. When the linearity condition is accomplished, the resulting plot exhibits an elliptical shape with a central symmetry with respect to its origin. If the response is not linear distortions of the elliptical shape are observed.[2] With the aim of adjusting this methodology for an IMPS measurement, we plotted the AC response output (in this case AC photocurrent), versus the AC perturbation input (AC light) to check the linearity of our response during IMPS measurements. Although the perturbation has to be small enough to assure a linear response, it has to be also large enough for being capable of detecting this response. The latter can be checked by using a resolution plot. For EIS measurements, this resolution plot shows the AC current and AC potential versus time. For an IMPS measurement, we can plot the AC perturbation together with the AC current response versus time to check the signal/response ratio. In Figure S1 a summary of the procedure followed for IMPS measurement validation is shown. Prior to the measurement, short circuit photocurrent under bias illumination is measured versus time for 120 seconds (Figure S1a).

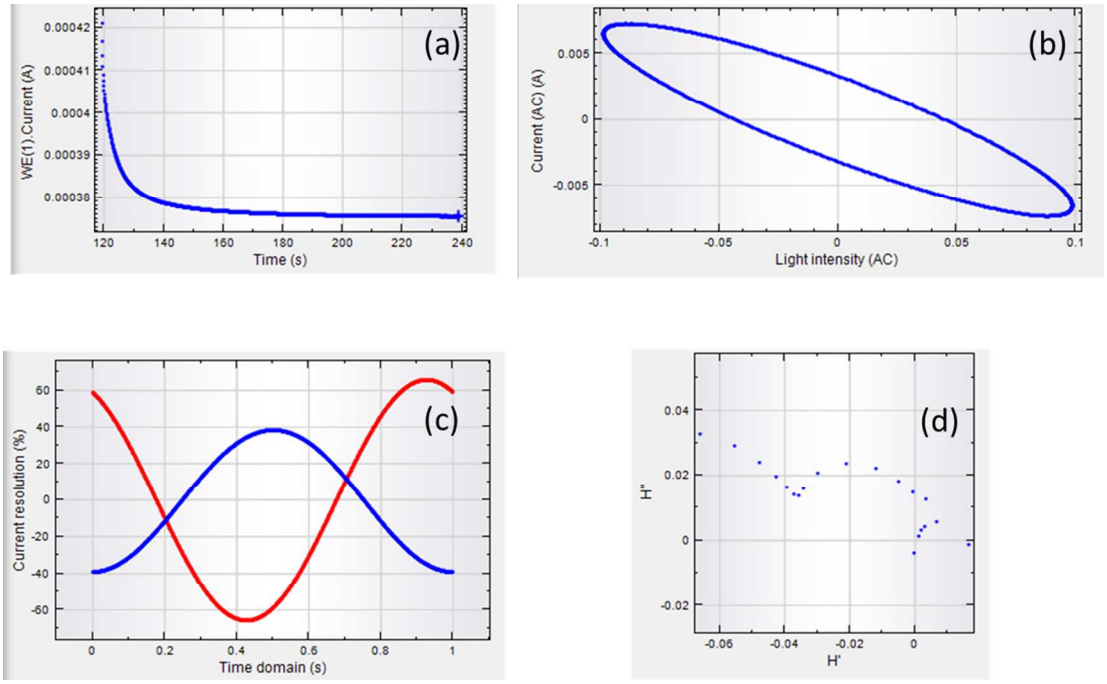

Figure S1 IMPS measurement of a cell of Configuration 1 (Table 1) with a perturbation of 5% of the DC light. a) Current versus time under LED illumination, b) Lissajous plot at $2 \cdot 10^2$ Hz , c) AC light illumination (red) and AC current response (blue) versus time, d) IMPS spectrum from 10^6 to $2 \cdot 10^2$Hz.

During IMPS measurement, resolution plot and Lissajous plot are checked to study linearity and causality. In Figure S1b we can observe an example of a Lissajous plot during an IMPS measurement for a perovskite cell when the perturbation amplitude is 5% relative to the illumination bias. This plot helps us to verify that the response to the applied amplitude complies with the linearity condition along the frequency range analyzed. A symmetrical plot is observed in all the frequency range, and its shape changes from a straight line to an ellipse depending on the phase shift. Figure S1c exhibits an example of a resolution plot at a defined frequency and Figure S1d the obtained IMPS spectrum.

To further check if we are using proper perturbation amplitude we measured the IMPS response at two different perturbation amplitudes: 5% and 0.5%. If the response is linear, the IMPS spectra must be independent of the perturbation amplitude. We observe that for both perturbations the response is the same, (see Figure S2).

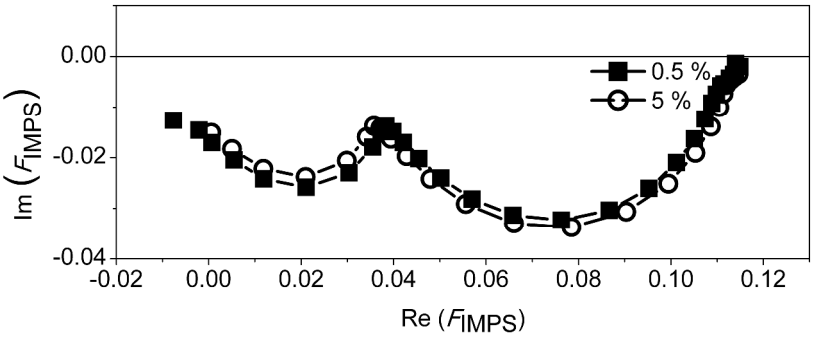

Figure S2 IMPS spectra for a Cell of configuration 1 (Table 1), measured under two different perturbation frequencies.

In Figure S3 we can see an example of the non-linear response observed when a much higher (25%) perturbation is used. For IMVS we checked the AC amplitude of the voltage instead of the current and we found the response was not similar when the perturbation was 0.5 or 5%, so we chose the lower perturbation frequency for the measurements, and always checked the linearity of the response.

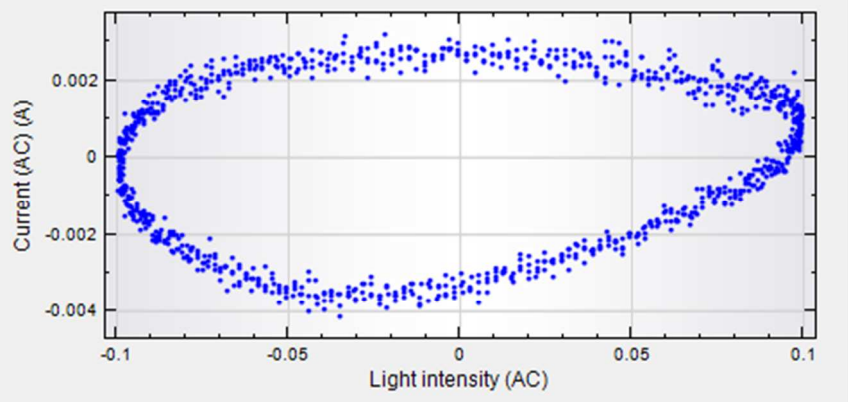

Figure S3 Lissajous plot of a cell of Configuration 1 with nonlinear response.

Electrochemical impedance spectroscopy of perovskite solar cells

Different equivalent circuits were used for the fitting depending on the features appearing in the spectra. *Rs* stands for the series resistance of the cell. Good fitting were obtained using RC elements for the high, intermediate and low frequency parts of the spectra. Capacitors were substituted by constant phase elements. When the transmission line is observed in the spectrum, RC element at intermediate frequencies is substituted by the distributed element DX1, comprising the charge transfer resistance at intermediate frequencies (R_{mf}), the capacitance at intermediate frequencies (C_{mf}), and the transport resistance (Rt).

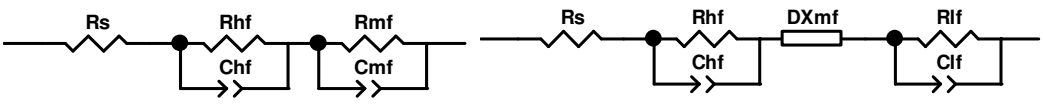

Figure S4 Equivalent circuits used for EIS fitting

In Figure S5 the main fitting parameters are plotted as a function of the potential. At high frequencies, the response of the back contact shows up in the spectrum (Au/HTM interface)[3] and also it has been suggested that it can be affected by transport in the perovskite.[4] Although considered in the fitting, high frequency features have not been included in the analysis. The increase of the capacitance obtained at intermediate frequencies is not as pronounced as in the liquid based DSSC devices. There is no consolidated interpretation about the origin of this capacitance in the literature.

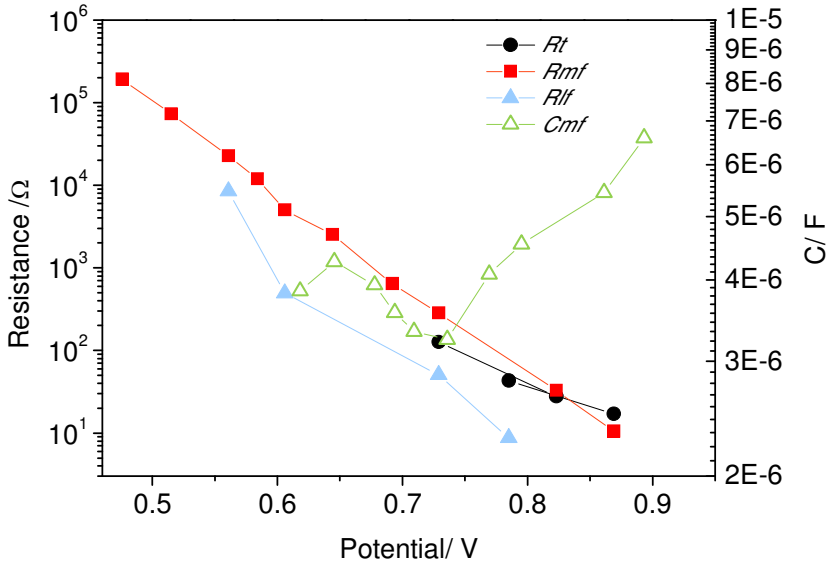

Figure S5 Fitting parameters obtained from EIS measurements at different open circuit potentials induced by illumination: *Rt*, transport resistance obtained for transmission line observed in the spectra, *Rmf* and *Rlf* charge transfer resistance obtained from the feature at mid and low frequency respectively, and *Cmf*, capacitance at mid frequency.

In less efficient cells, an extra feature appearing between high and mid frequencies is observed at intermediate voltages.

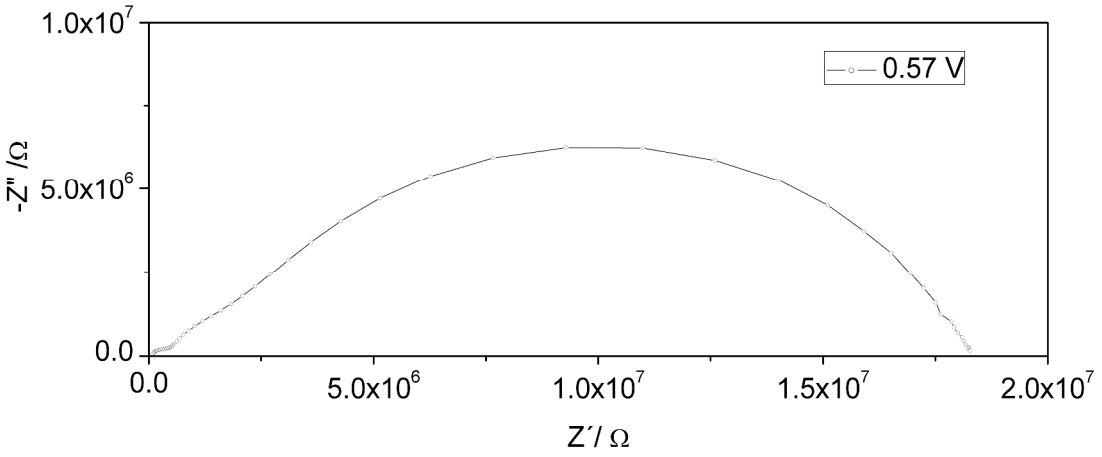

Figure S6 Nyquist plot of a PS solar cell (one step deposition), measured at open circuit under illumination. The PCE efficiency of the cell under one sun illumination was 3.4%

Electron lifetime of perovskite solar cells

During fitting procedure constant phase elements (CPE) with relatively low ideality factors are required to achieve a good match between the equivalent circuit simulation and the experimental response, and the capacitance is then obtained taking into account the CPE ideality factor. Importantly, considering this ideality factor into account we ensure that IMVS and EIS lifetime coincide (Figure S7).

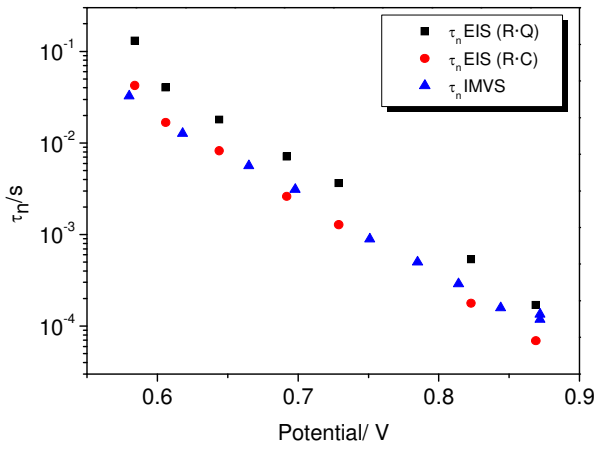

Figure S7 Comparison of electron lifetimes obtained from IMVS with those obtained from EIS without taken into account the ideality factor (Q), or calculating the capacitance as $\mathbf{C} = \frac{(\mathbf{QR})^{\mathbf{1/n}}}{\mathbf{R}}$, where *R* is the charge transfer resistance at intermediate frequencies, and *n* is the ideality factor.

Reconstruction of the IV curve from small-perturbation measurements

Eq. 8 is solved by means of the Forward Time Centered Space (FTCS) method with the following boundary conditions:[5]

$$n(x=0,t)=n_0(V)$$

$$n(x,t=0)=n_0(V) \qquad \text{S1}$$

$$\left(\frac{d\,n(x,t)}{dx}\right)_{x=d}=0$$

Where *d* is the thickness of the active layer, *V* is the applied voltage and

$$n_0(V) = n_0^0 \exp(V/k_B T) \qquad \text{S2}$$

The generation term G is calculated as

$$G(x) = F \int_{\lambda_{min}}^{\lambda_{max}} I_o(\lambda) \epsilon_{cell}(\lambda) \exp\left[-\epsilon_{cell}(\lambda) x\right] d\lambda \; ; \qquad \text{S3}$$

where $I_0(\lambda)$ is the solar spectrum (here taken from the standard AM1.5G) and $\varepsilon_{cell}(\lambda)$ is the absorption coefficient of the perovskite film in the solar cell.[6] F is a prefactor that accounts for the overall absorption and efficiency of electron-hole pair generation in the active film.

Once the equation is solved the photocurrent density for a given value of the voltage V is obtained from the stationary density profile at x = 0 (it is assumed that collection of electrons and holes in external contacts is the same):

$$J(V) = \left(\frac{d\, n(x,t)}{dx} \right)_{x=0,\, t \to \infty} \qquad \text{S4}$$

Solving Eq.8 for different values of V, and using Eq. S2 and Eq. S4, the full JV-curve can be obtained. In the procedure,[5–7] F is adjusted so that the experimental short-circuit photocurrent of the solar cell is reproduced. On the other hand, the recombination constant k_0 is adjusted so that the photocurrent is zero at $V = V_{oc}$ where V_{oc} is the experimental open-circuit photovoltage.

The impact of a series resistance, R_s in the model is introduced in the following way: the voltage V entering eq A-3 is replaced by $V = V + JAR_s$, where J is the current density and A the geometrical surface area. The continuity equation is solved for this new voltage, and the new current obtained is utilized to modify the voltage. The process is repeated until consistency between successive values of J is achieved for a fixed value of R_s. The original value of R_s is obtained from fitting the experimental current at the maximum power point of the IV curve.

The following parameters were used in the calculations: $D_0 = 10^{-10}$ cm^2s^{-1} (electron diffusion coefficient for electrons/holes),[8] $n_0^0 = 10^{15}$ cm^{-3} (electron density at zero bias)[9] and d = 0.5 μm (thickness of the active layer PS/TiO2).[10]

Results for two choices of the β parameter, with and without series resistance are shown in Figure S8.

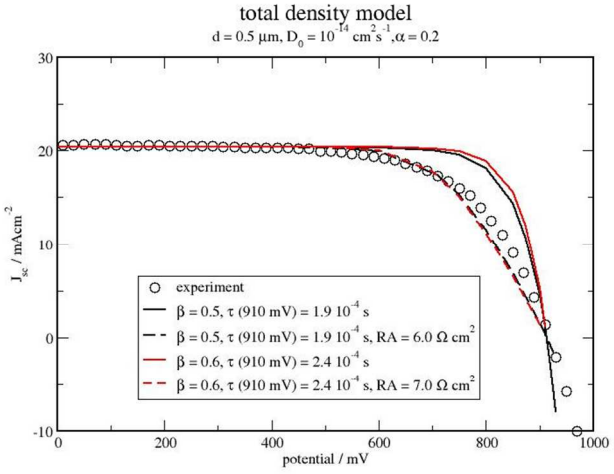

Figure 8 JV curves for tow choices of the β parameter, with and without series resistance (R). A is the geometrical area.

References

(1) Lvovich, V. F. *Impedance Spectroscopy : Applications to Electrochemical and Dielectric Phenomena*; Wiley: Somerset, NJ, USA, 2012.

(2) Orazem, M. E.; Tribollet, B. *Electrochemical Impedance Spectroscopy*; 2011th ed.; John Wiley & Sons.

(3) Juárez-Pérez, E. J.; Wu, M.; Fabregat-santiago, F.; Lakus-wollny, K.; Mankel, E.; Mayer, T.; Jaegermann, W.; Mora-Seró, I. Role of the Selective Contacts in the Performance of Lead Halide. *J. Phys. Chem. Lett.* **2014**, *5*, 680–685.

(4) Dualeh, A.; Moehl, T.; Tétreault, N.; Teuscher, J.; Gao, P.; Nazeeruddin, M. K.; Grätzel, M. Impedance Spectroscopic Analysis of Lead Iodide Perovskite-Sensitized Solid-State Solar Cells. *ACS Nano* **2014**, *8*, 362–373.

(5) Anta, J. A.; Casanueva, F.; Oskam, G. A Numerical Model for Charge Transport and Recombination in Dye-Sensitized Solar Cells. *J. Phys. Chem. B* **2006**, *110*, 5372–5378.

(6) Lee, M. M.; Teuscher, J.; Miyasaka, T.; Murakami, T. N.; Snaith, H. J. Efficient Hybrid Solar Cells Based on Meso-Superstructured Organometal Halide Perovskites. *Science* **2012**, *338*, 643–647.

(7) Villanueva-Cab, J.; Oskam, G.; Anta, J. A. A Simple Numerical Model for the Charge Transport and Recombination Properties of Dye-Sensitized Solar Cells: A Comparison of Transport-Limited and Transfer-Limited Recombination. *Sol. Energy Mater. Sol. Cells* **2010**, *94*, 45–50.

(8) Stranks, S. D.; Eperon, G. E.; Grancini, G.; Menelaou, C.; Alcocer, M. J. P.; Leijtens, T.; Herz, L. M.; Petrozza, A.; Snaith, H. J. Electron-Hole Diffusion Lengths Exceeding 1 Micrometer in an Organometal Trihalide Perovskite Absorber. *Science* **2013**, *342*, 341–344.

(9) Anta, J. A.; Idígoras, J.; Guillén, E.; Villanueva-Cab, J.; Mandujano-Ramírez, H. J.; Oskam, G.; Pellejà, L.; Palomares, E. A Continuity Equation for the Simulation of the Current-Voltage Curve and the Time-Dependent Properties of Dye-Sensitized Solar Cells. *Phys. Chem. Chem. Phys.* **2012**, *14*, 10285–10299.

(10) Burschka, J.; Pellet, N.; Moon, S.-J.; Humphry-Baker, R.; Gao, P.; Nazeeruddin, M. K.; Grätzel, M. Sequential Deposition as a Route to High-Performance Perovskite-Sensitized Solar Cells. *Nature* **2013**, *499*, 316–319.